Structural parameters of the myelin transmembrane proteolipid in reverse micelles

B. P. Binks, D. Chatenay, C. Nicot,* W. Urbach,† and M. Waks*

Laboratoire de Spectroscopie Hertzienne de 1'E.N.S., 75231 Paris Cedex 05, France; *Unité de Recherche Associée au CNRS n° 586 à l'Université Paris V 75270 Paris Cedex 06, France; and †Laboratoire d'Imagerie Ultrasonore Médicale (CNRS UA 593) Université Paris V, CHU Cochin, 75674 Paris Cedex 14

ABSTRACT The Folch-Pi proteolipid is the most abundant structural protein from the central nervous system myelin. This protein-lipid complex, normally insoluble in water, requires only a small amount of water for solubilization in reverse micelles of sodium *bis* (2-ethylhexyl) sulfosuccinate (AOT) in isooctane. The characterization of the proteolipid-free and proteolipid-containing micelles was undertaken by light scattering and fluorescence recovery after fringe pattern photobleaching (FRAPP) experiments. Quasi elastic light scattering (QELS) was carried out at a high (200 mM) AOT concentration, at low water-to-surfactant mole ratio (w_o = 7) and at increasing protein occupancy. Two apparent hydrodynamic radii, differing tenfold in size, were obtained from correlation functions. The smaller one (R_H^a = 5.2 nm) remains constant and corresponds to that measured for protein-free micelles. The larger one increases linearly with protein concentration. In contrast, FRAPP measurements of self-diffusion coefficients were found unaffected by the proteolipid concentration. Accordingly, they have been performed at constant protein/surfactant mole ratios. The equivalent R_H, extrapolated to zero AOT concentration for protein-free reverse micelles (2.9 nm) and in the presence of the proteolipid (4.6 nm), do not reveal the mode of organization previously suggested by QELS measurements. The complex picture emerging from this work represents a first step in the characterization of an integral membrane protein in reverse micelles.

INTRODUCTION

The myelin sheath that is surrounded by successive spirals and insulates axons in the central nervous system, contains a unique set of structural proteins, probably involved in the extension and the compaction of its elaborate multilamellar architecture. The water-soluble basic protein (Mr = 18,500) is located within the cytoplasmic interlamellar aqueous spaces, while the exceptionally hydrophobic Folch-Pi proteolipid protein (Mr = 30,000) penetrates the bilayer with polar regions protruding into both the cytoplasmic and extracellular aqueous spaces (1).

Our previous work (2–4) has established that the myelin aqueous spaces reveal a number of physicochemical properties similar to those of reverse micelles. These self-organized, thermodynamically-stable assemblies of sodium *bis* (2-ethylhexyl) sulfosuccinate (AOT), water and isooctane, have been used for the insertion and study of myelin proteins in a membrane-mimetic environment. Recently, we have shown that, for optimal micellar solubilization, the water-insoluble proteolipid requires (*a*) an unusually high AOT concentration (200 mM) suggesting the involvement of more than one micelle per protein molecule, (*b*) a small amount of water in the w_o = $[H_2O]/[AOT]$ = 5–7 range, (*c*) a definite number (6 ± 1 moles) of tightly-bound acidic lipids per mole of protein (5). More importantly, under such experimental conditions, the protein retains a stable conformation and a specific degree of periodicity in structure (55% α-helix) compatible with recent models of the transmembrane protein (6, 7).

Earlier, Wolman and Wiener (8) described the formation of water-in-oil (hexagonal) emulsions of myelin membranes, depending on the chemical nature of ions present. These experiments point to the possibility of reverse micellar structures in biological membranes. Owing to the possible role of the proteolipid in the organization of myelin (or in its destruction in demyelinating processes), the primary focus of this work is to investigate the configuration of such a peculiar protein-micelle system. Because experimental data about the size, shape, and other parameters of reverse micelles are scarce at high surfactant concentration, we report the first attempt to evaluate the size of proteolipid-containing (relative to proteolipid-free) reverse micelles. Recent observations (9) have pointed out that such an investigation requires the use of complementary techniques. Accordingly, we have carried out light scattering experiments in conjunction with fluorescence recovery after fringe pattern photobleaching (FRAPP) measurements in order to examine, from an estimation of the respective structural parameters, a possible organization of the

Please address reprint requests to W. Urbach. B. P. Binks present address is School of Chemistry, University of Hull, Hull H46 TRX, England.

0006-3495/89/05/949/07 $2.00

proteolipid in a membrane-mimetic environment. Because the Folch-Pi proteolipid is to date the only transmembrane protein solubilized in reverse micelles of AOT so far reported (2), it is also hoped that this work will extend our knowledge on the behavior of biologically important membrane proteins or enzymes active at interfaces.

MATERIALS AND METHODS

Chemicals

Sodium *bis*(2-ethylhexyl) sulfosuccinate (AOT), a gift from the Cyanamid Co., France, was purified according to Wong et al. (10) and carefully dried in vacuo. Fluorescein isothiocyanate isomer I (FITC) was from Sigma Chemical Co., St Louis, MO. *N*-acetylglycyl-*L*-lysine methyl ester acetate was purchased from Serva Fine Biochemicals Inc., Heidelberg, FRG. All the organic solvents were from Merck (Darmstadt, FRG). Isooctane was Uvasol grade, chloroform and methanol were Pro Analysi grade. All other chemicals were from the best available sources.

Protein

A total lipid extract containing the proteolipid was obtained according to Lees and Sakura from bovine white matter (11). The proteolipid was precipitated by a dropwise addition of isooctane (6 vol) to 1 vol of a chloroform and methanol (2:1, vol:vol) solution. The lipid composition and the thiol group titer of the proteolipid were determined precisely. The detailed results of these investigations are reported elsewhere (5).

Micellar solubilization

The precipitate was solubilized by a preformed micellar solution, at a reasonably high AOT concentration (200 mM) and at $w_o = 7.0$ (Fig. 1). Some micellar solutions were prepared with pure (MilliQ) water, other for FRAPP experiments with 0.1 M borate, pH 9.5. Solubilization of the proteolipid was achieved by vigorous stirring, after a 2 min sonication (5).

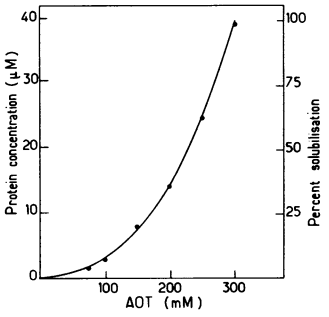

FIGURE 1 Solubilization of the Folch-Pi proteolipid in reverse micelles as a function of AOT concentration, at $w_o = 7.0$. Each experimental point represents a separate experiment at a given concentration of surfactant.

Labeling with FITC

The reaction of the dipeptide *N*-acetylglycyl-*L*-lysine methyl ester acetate with FITC was carried out as detailed in a previous publication (9). This procedure could not be employed for the labeling of the water-insoluble proteolipid. A new procedure was therefore devised. The isooctane precipitate of the proteolipid was first dissolved in a 2:1 chloroform-methanol solution and its concentration determined in the same solvent. For each mole of protein, 2 or 3 molar equivalents of a 25 mM 2:1 chloroform-methanol solution of isothiocyanate were added, left at 20°C for 3 h with slow mixing and left overnight at 0°C. The solution was then twice precipitated by isooctane, the excess label being removed with the supernatant. The labeled precipitate was finally solubilized in micellar solutions under the above experimental conditions. Fluorescence polarization measurements were carried out on a XE 450 apparatus (SLM Instruments Inc., Urbana, IL). The binding of the fluorescent dye to the proteolipid was verified by fluorescence polarization measurements of the free and bound dye in reverse micelles. As expected, the polarization P increased from $P = 0.20$ for free FITC in micellar solutions to $P = 0.32$ for FITC bound to the proteolipid solubilized in micellar solutions, indicating a decreased mobility of the fluorophore.

Instrumental measurements

The absorption spectra of the optically transparent micellar solutions were measured on a CARY 118 spectrophotometer. For the proteolipid, a millimolar extinction coefficient of 40.5 cm^{-1} was used, at 278 nm. For the labeled proteolipid, a millimolar extinction coefficient of 72 cm^{-1} was taken at 497 nm, at pH 9.5 (12). The amount of solubilized labeled protein was calculated from the absorption spectrum at 278 nm taking into account the measured FITC millimolar contribution (30.0 cm^{-1}). The extent of labeling was calculated from absorption measurements; it was in the 0.2–0.5 molar range of FITC per mole of protein. Analysis by thin layer chromatography (TLC) of the lipids extracted from the proteolipid (5) did not show any fluorescent lipid spot indicative of lipid labeling.

Dynamic light scattering

QELS experiments allow the determination of both the size and polydispersity of small aggregates, and characterization of the interaction between them (13). The experiments have been performed using a laboratory built autocorrelator, interfaced to a HP 9835 computer allowing the continuous control of the baseline. The problem of dust particles disturbing the measurements has been solved by introducing a check procedure: at the end of each run, the calculated baseline was compared with the value measured using delay channels. If the discrepancy was >0.2%, the data were rejected. The light source was an Ar^+ laser ($\lambda = 514.5$ nm). The scattered intensity autocorrelation function, $g^{(2)}(t)$, was measured in 112 points grouped in four zones with different sampling times. This allows the precise determination of both the short time and the asymptotic behavior ($t \rightarrow \infty$) of $g^{(2)}(t)$ in the same run. For monodisperse, identical particles $g^{(2)}(t)$ decays exponentially with a single characteristic time $\tau = (2q^2D_c)^{-1}$, where D_c is the collective diffusion coefficient for Brownian motion, $q = 4\pi/\lambda \, n \sin(\theta/2)$ is the scattering wave vector, θ the scattering angle and n the refractive index of the medium. For moderately polydisperse samples, the correlation function deviates from exponential shape according to (14):

$$g^{(2)}(t) = A[e^{-t/\tau + p/2(t/\tau)^2}]^2.$$

The polydispersity index p is related to the width of the size distribution. As before τ scales with q^{-2} and a value of D_c is obtained.

In the more concentrated protein-containing samples a two exponen-

tial fit was attempted to describe $g^{(2)}(t)$. The characteristic times τ_1 and τ_2 ($\tau_2 \gg \tau_1$) scale and q^{-2}.

Static light scattering

If the aggregates are sufficiently large to produce an angular dependence of scattered intensity, one may deduce aggregate shape from $I(\theta)$ dependence. In our case this dependence was measured as the dissymetry ratio (15): $d(\theta) = I(\theta)/I(\pi - \theta)$ and the experimental results were fitted to the theoretical predictions for various structures (16) as mentioned below.

Fluorescence recovery after fringe pattern photobleaching (FRAPP)

This technique allows measurement of the self-diffusion coefficient D_s of fluorescent probes. When strongly illuminated, these probes irreversibly lose their fluorescent properties (photobleaching). In the illuminated volume, the fluorescence intensity is measured afterwards by use of a low intensity light beam. The signal increases as new probes enter the studied volume and D_s is deduced from the recovery time. The set-up has been described previously (9). The recovery curves were fitted to the expression

$$I(t) = Ae^{-t/\tau} + B,$$

where $\tau = i^2/4\pi^2 D_s$ and i is the fringe spacing. For each sample, we verified that τ^{-1} scaled with q^2 (= $[2\pi/i]^2$) and D_s was obtained from the τ^{-1} versus q^2 plot. Typical fringe spacings were in the range 10–100 μm.

RESULTS AND DISCUSSION

Protein free systems

Dynamic light scattering experiments have been carried out on a series of reverse micellar solutions of AOT of differing concentrations but at a constant value of $w_0 = 7$. The results are presented in Fig. 2 both in terms of the measured diffusion coefficient D_c and the apparent hydrodynamic radius R_H^a given by the Stokes-Einstein relation:

$$R_H^a = \frac{kT}{6\pi\eta D_c},$$

where k is the Boltzman constant and η the continuous phase viscosity (0.491 cP for isooctane). An assumption made during dilution is that the composition of the aggregates remains unchanged. The polydispersity index was in the range 1 to 10% for all the samples studied.

At low volume fractions Φ (<0.07), the variation of D_c with Φ may be written:

$$D_c = D_0(1 + \alpha\Phi),$$

where D_0 is the infinite dilution value of D_c and α the first virial coefficient reflecting both direct and hydrodynamic particle interactions (for hard spheres, $\alpha = 1.5$). Our results yield $\alpha \simeq -7$, suggesting attractive interactions (13,17) but these are not strong enough to lead to critical behavior and phase separation. At higher Φ (>0.07), the form of the curve is similar to that obtained with other systems and, at least qualitatively, well understood (13,18,19).

For micellar volume fractions <0.02, the scattered intensity was fairly low and statistical accuracy in the measured correlation functions was limited. This is because, for $w_0 = 7$, the droplet size is small and the index matching between the continuous phase and droplets is good. A large uncertainty exists in the measured D_c (5%), despite averaging values at different angles, and hence in the determination of D_0. A similar problem was reported by Abery et al. (17) even at higher w_0 values. Taking this into account, the data lead to an R_H value between 2.5 and 3 nm. This result being imprecise, we have used the FRAPP technique. As already described in a previous paper (9), FRAPP experiments allow the measurement of protein-free micellar R_H after the solubilization of a fluorescent dipeptide (see Materials and Methods). In Fig. 3, we present the variation of the measured self-diffusion coefficient with Φ determined by this technique. This can also be described by a relation of the form:

$$D_s = D_0(1 + \beta\Phi),$$

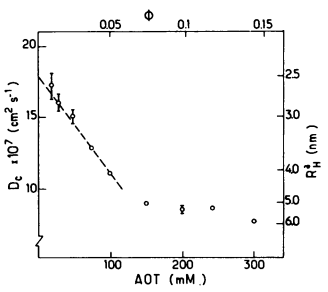

FIGURE 2 QELS experiments of protien-free micelles. D_c or apparent hydrodynamic radius R_H^a versus AOT concentration or volume fraction (Φ).

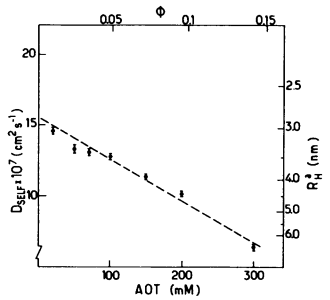

FIGURE 3 FRAPP experiments of dipeptide containing micelles. D_{self} or R_H^a versus AOT concentration or volume fraction (Φ). R_H extrapolates to 2.9 nm, at zero AOT concentration.

where β is the first virial coefficient; contrary to D_c, no strong dependence of D_s upon direct interactions is expected (19). The D_0 value of $15.2 \cdot 10^{-7}$ cm^2 s^{-1} leads to a hydrodynamic radius of 2.9 nm, in good agreement with values reported in the literature using different techniques (20).

Protein-containing systems

The aim of this study was to investigate the effect of increasing concentrations of protein on the structure of the reverse micellar system. In order to dissolve reasonably different quantities of proteolipid, it was necessary to fix the AOT concentration at 200 mM, because this corresponded to a satisfactory solubilization capacity of the system (Fig. 1).

Results of QELS experiments are shown in Fig. 4 in terms of R_H^a versus micromoles of solubilized protein. It is possible to distinguish two regimes in Fig. 4, at protein concentration $S < 5$ μM, the correlation function was analyzed with a single exponential plus cumulant program. Only one characteristic time, τ, was obtained, and the value of D_c was independent of the protein concentration. This corresponds to an apparent hydrodynamic radius of 5.2 ± 0.1 nm. It may be compared with $R_H^a = 5.2$ nm for protein-free micelles calculated from the diffusion coefficient value at the same AOT concentration (200 mM) in Fig. 2. It must be recalled that dynamic light scattering is a global measurement, so that the resulting R_H^a values are an average of protein-free and protein-containing radii (4). However, for the weak protein concentration (compared with surfactant), this distribution of sizes is displaced towards the empty droplets. In more concentrated protein-containing samples (>5 μM), experimental curves were analyzed using a maximum entropy fitting procedure (21). This allowed us to extract two main apparent hydrodynamic radii. The larger value increases linearly with protein concentration while the smaller radius remains constant and equal to 5.2 nm. These results seem to suggest that the medium is predominantly composed of empty reverse micelles and larger structures containing protein.

In order to gain information about protein-containing structures, we have used FRAPP which allows exclusively the size determination of protein-containing micelles. FRAPP experiments were performed at two protein concentrations (in the 4 μmol to 15 μmol range) at a finite AOT concentration of 200 mM and a w_0 value of 7.0 (Fig. 5). At both concentrations, we find a diffusion coefficient of comparable value, corresponding to an apparent average hydrodynamic radius ~10 nm, indicating that the measurements are unaffected by the protein concentration. We have therefore performed FRAPP experiments at decreasing AOT concentrations and a single protein/surfactant ratio, in order to obtain a R_H value at zero AOT concentration. Fig. 6 illustrates the results of these experiments: R_H extrapolates to 4.6 nm.

The picture emerging from the structural study appears to be that upon increasing the protein concentration, large protein-micelle aggregates are formed in equilibrium with the initial size reverse micelles. Such aggregates are only observed by light scattering experiments. They do not originate from the oxidation of the protein SH groups (22) because all the sulfhydryls of the proteolipid remain titratable in reverse micelles (5). In contrast, FRAPP experiments do not reveal structures of equiva-

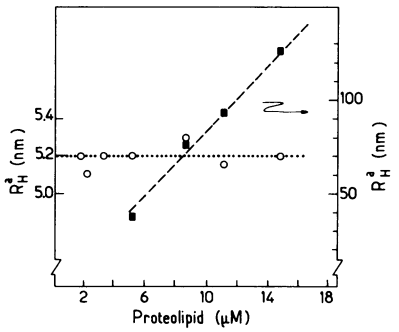

FIGURE 4 Protein-containing micelles. R_H^a deduced from QELS experiments versus protein concentration at [AOT] = 200 mM and w_0 = 7.0. (*Left hand ordinate*) Low R_H^a: ○ (*right hand ordinate*) High R_H^a: ■.

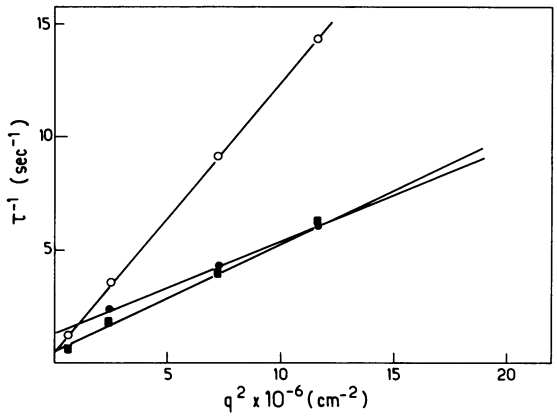

FIGURE 5 FRAPP experiments. D_s determination from $\tau^{-1} = D_s q^2$ plot for protein-free (○) and protein-containing solutions 5 μM: (■) and 15.8 μM: (●). It may be noticed that the curves do not pass through the origin. This is due to the fact that the second weaker incident laser beam may continue to bleach. In this case, one may write $\tau^{-1} = D_s q^2 + \tau_o^{-1}$, where τ_o^{-1} is given for $q = 0$. It is possible to reduce τ_o^{-1} to zero by diminishing the intensity of the incident beam, but the signal would become too weak. An alternative would consist in making the protein more fluorescent, but this proved to be difficult.

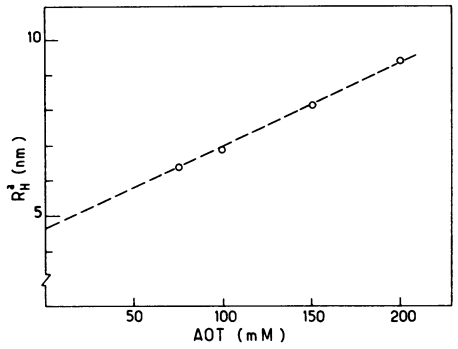

FIGURE 6 R_H^a obtained from FRAPP experiments versus AOT concentration. At zero AOT concentration, R_H extrapolates to 4.6 nm [AOT]/[PROTEIN] = 3×10^4.

lent size; furthermore, all the recovery curves were perfectly fitted with a single exponential (Fig. 7). The curve does not even permit one to guess the presence of larger aggregates. In fact, the two types of results are not in contradiction. Indeed, the population of larger objects is probably too small to be observed in FRAPP experiments. Their low concentration is further confirmed by the measurements of the bulk viscosity carried out using a Ubbelohde-type viscometer in the total range of protein concentration studied, this viscosity remained constant. In the light scattering experiments, the scattered intensity by these larger structures is more important because it is proportional to R^6, where R is the size of the scattering object (16).

The question remains as to the possible organization of the large aggregates. An idea may be obtained from the results of the static study measuring the anisotropy of the particles. Theoretical expressions have been developed to interpret such data for structures of different shapes (15,16) e.g., spheres, rods, and random coils. Typical anisotropy results are presented in Fig. 8 for a protein-containing system (11 μM). Also given are the fits to the theory describing spheres and monodisperse random coils. The best agreement between the experimental results and theory have been obtained with a structure of random coils. However, it is agreed that the interpretation of these data may be equally acceptable with other aggregate shapes like flexible rods or polydisperse spheres.

CONCLUSION

If we consider all the results together, a tentative model for the solubilization of Folch-Pi proteolipid into a reverse micellar system may be proposed. At low protein concentration, in addition to protein-free micelles (R_H = 2.9 mm), there exist, in equilibrium, micelle-protein structures of R_H = 4.6 nm. These structures would be formed by two opposed micellar caps covering the hydrophilic regions of one proteolipid molecule and linked by a bundle of 4 or 5 hydrophobic helices (6,7) in contact with isooctane, as suggested in Fig. 9. As further protein is added, the number of such structures would increase and then begin to aggregate, due to increased protein–protein intermicellar interactions. A more elaborate organisation appears then, which may be represented as a random coil arrangement. Although clearly speculative, such a model resembles that proposed by Ramakrishnan et al. (23), as resulting from small angle x-ray scattering studies of rhodopsin incorporated into phospholipid-hexane reverse micelles.

Under very different experimental conditions, the val-

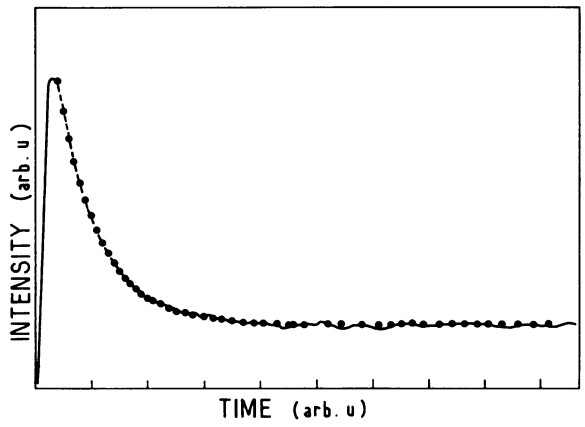

FIGURE 7 FRAPP Experiments. Typical plot of fluorescence intensity versus time for protein-containing micelles. Protein concentration; 15 μM. Experimental values (---), fit (·) AOT concentration, 200 mM.

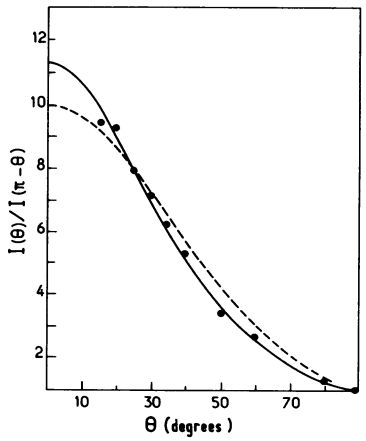

FIGURE 8 Static Light Scattering experiments. The dissymmetry ratio $I(\theta)/I(\pi - \theta)$ versus the scattering angle θ. Experimental points (·), random coil fit (—), sphere fit (---).

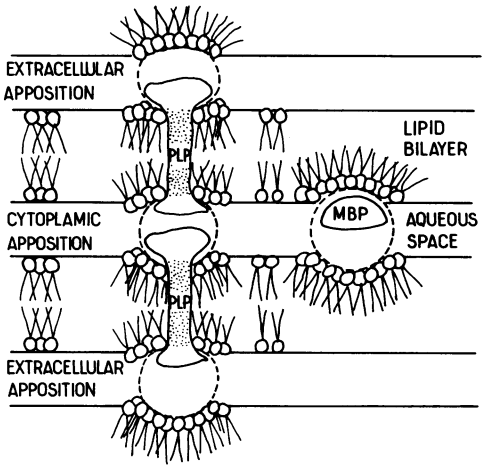

FIGURE 9 Schematic representation of myelin aqueous spaces. MBP: myelin basic protein, PLP: proteolipid. Dashed circles underline the analogy with the structure of reverse micelles. The dotted parts of the proteolipid represent the intramembranous domains consisting of several hydrophobic α helices.

ues of the delipidated proteolipid protein's gyration radius within lipid vesicles have been extensively reviewed and discussed (24). The present investigation has been carried out on a proteolipid micellar solution in isooctane. It thus seems inappropriate to compare the hydrodynamic radii reported here for a lipid-protein complex with size parameters in the literature for the lipid depleted protein, even more so that interactions with the micelles are also included. Furthermore, we have shown elsewhere (5) that, upon delipidation, the protein undergoes an alteration which prevents its incorporation into reverse micelles, even after readdition of the missing lipid. In the present study we had thus to face a brand new situation.

The incorporation of water-soluble proteins in reverse micelles and the subsequent perturbations introduced in the system are now fairly well documented (9, 25). Although the water-shell model (26) obviously requires further modifications, it still remains useful to describe the properties of the encapsulated proteins (4). In contrast to individual macromolecules solubilized within aqueous droplets described so far, we are dealing with a water-insoluble protein-lipid complex which exhibits distinct hydrophobic and charged regions. The interactions at the peptide level can therefore occur with two types of environments, the micellar encased water and with the hydrocarbon phase. Moreover, the high surfactant concentrations required for the incorporation of the proteolipid, increase attractive interactions as a function of protein concentration and lead to aggregated structures.

Because of the diversity of proteins, many patterns of interaction with reverse micelles can be expected. This work thus represents the first attempt to elucidate the nature and the mechanism of a more intricate micellar organization than so far reported for other proteins (27). Our results suggest that the mode of organization of the myelin proteolipid in reverse micelles is compatible with the dual microenvironment experienced by the transmembrane protein in myelin, where it interacts both with the lipid bilayer and the interlamellar aqueous spaces (Fig. 9). They are also consistent with recent observations suggesting complex and extensive protein–protein associations among myelin components (28).

Dr. P. B. Binks wishes to thank the Royal Society for the award of a Research Fellowship under the European Science Exchange Program. This work was supported in part by grants from Institut National De La Sante Et De La Recherche Medicale (grant 889015) and from Association Francaise Contre les Myopathies to M.Waks.

Received for publication 22 April 1988 and in final form 24 October 1988.

REFERENCES

1. Lees, M. B. and S. W. Brostoff. 1984. Myelin Proteins in Myelin. P. Morell, editor. Plenum Publishing Corp., New York. 197–209.
2. Delahodde, A., M. Vacher, C. Nicot, and M. Waks. 1984. Solubilization and insertion into reverse micelles of the major myelin transmembrane proteolipid. *FEBS (Fed. Eur. Biochem. Soc.) Lett.* 172:343–347.
3. Nicot, C., M. Vacher, J. Gallay, and M. Waks. 1985. Membrane proteins in reverse micelles: myelin basic protein in a membrane-mimetic environment. *Biochemistry.* 24:7024–7032.
4. Chatenay, D., W. Urbach, A. M. Cazabat, M. Vacher, and M. Waks. 1985. Proteins in membrane-mimetic systems. Insertion of myelin basic protein into microemulsion droplets. *Biophys. J.* 48:893-898.
5. Vacher, M., M. Waks, and C. Nicot. 1989. Myelin proteins in membrane mimetic systems. Tight lipid association required for insertion of the Folch-Pi proteolipid into reverse micelles. *J. Neurochem.* 52:117–123.
6. Stoffel, W., H. Hillen, W. Schröder, and R. Deutzmann. 1983. The primary structure of bovine brain myelin lipophilin (proteolipid apoprotein). *Hoppe-Seyler's Z. Physiol. Chem.,* 364:1455–1466.
7. Laursen, R. A., M. Samiullah, and M. B. Lees. 1984. The structure of bovine brain myelin proteolipid and its organization in myelin. *Proc. Natl. Acad. Sci. USA.* 81:2912-2916.
8. Wolman, M., and H. Wiener. 1965. Structure of the myelin sheath as a function of concentration of ions. *Biochem. Biophys. Acta.* 102:269–272.
9. Chatenay, D., W. Urbach, C. Nicot, M. Vacher, and M. Waks. 1987. Hydrodynamic radii of protein-free and protein-containing reverse micelles as studied by fluorescence recovery after fringe photobleaching. Perturbations introduced by myelin basic protein. *J. Phys. Chem.* 91:2198–2201.

10. Wong, M., J. K. Thomas, and M. Grätzel. 1976. fluorescence probing of inverted micelles. The state of solubilized water clusters in alkane/diisoocytl Sulfosuccinate (Aerosol OT) solution. *J. Am. Chem. Soc.* 98:2391–2397.

11. Lees, M. B., and J. D. Sakura. 1978. Preparation of proteolipids. *In* Research Methods in Neurochemistry. N. Marks and R. Rodnight, editor. Plenum Publishing Corp., New York. 345–376.

12. Garel, J. R. 1976. pk changes of ionizable reporter groups as an index of conformational changes in proteins. *Eur. J. Biochem.* 70:179–189.

13. Cazabat, A. M., and D. Langevin. 1981. Diffusion of interacting particles: light scattering study of microemulsions. *J. Chem. Phys.* 74:3148–3152.

14. Pusey, P. N. 1973. Photon Correlation and Light Beating Spectroscopy. H. Z. Cumins and E. R. Pike, editors. Plenum Publishing Corp. New York.

15. Young, C. Y., P. J. Missel, N. A. Mazer, G. B. Benedek, and M. C. Carey. 1978. Deduction of micellar shape from angular dissymetry measurements of light scattered from aqueous SDS solutions. *J. Phys. Chem.* 82:1375–1379.

16. Berne, B. J., and R. Pecora. 1976. Dynamic Light Scattering. John Wiley and Sons Inc., New York.

17. Albery, W. J., R. A. Choudery, N. Z. Atay, and B. H. Robinson. 1987. Rotating diffusion cell studies of microemulsion kinetics. *J. Chem. Soc. Faraday Trans.* I. 83:2407–2419.

18. Chatenay, D., W. Urbach, A. M. Cazabat, and D. Langevin. 1985. Onset of droplet aggregation from self-diffusion measurements in microemulsions. *Phys. Rev. Lett.* 54:2253–2256.

19. Chatenay, D., W. Urbach, R. Messager, and D. Langevin. 1987. Self-diffusion of interacting micelles: FRAPP study of micelles self-diffusion. *J. Chem. Phys.* 86:2243–2351.

20. Robinson, B. H., C. Toprakcioglu, J. C. Dore, and P. Chieux. 1984. Small angle neutron-scattering study of microemulsions stabilized by Aerosol-OT. *J. Chem. Soc. Faraday Trans. I.* 80:13–27.

21. Gill, S. F., and J. Skilling. 1985. Algorithms and applications. *In* Maximum Entropy and Bayesian Methods in Inverse Problems. C. R. Smith and W. T. Grandy, editors. 83–132.

22. Vacher, M., M. Waks, and C. Nicot. 1984. The thiol groups of the Folch-Pi protein from bovine white matter. *Biochem. J.* 218:197–202.

23. Ramakrishnan, V. R., A. Darszon, and M. Montal. 1983. A small-angle x-ray scattering study of a rhodopsin-lipid complex in hexane. *J. Biol. Chem.* 258:4857–4860.

24. Boggs, J. M., M. A. Moscarello, and D. Papahdjopoulos. 1982. Lipid-protein interactions in myelin. *In* Lipid-Protein Interactions. P. C. Jost and O. M. Griffith, editors. John Wiley and Sons, Inc., New York 1–51.

25. Luisi, P. L., and L. J. Magid. 1986. Solubilization of enzymes and nucleic acids in hydrocarbon micellar solutions. *CRC Crit. Rev. Biochem.* 20:409–474.

26. Bonner, F. J., R. Wolf, and P. M. Luisi. 1980. Micellar solubilization of biopolymers in hydrocarbon solvents. I. A Structural Model for Protein-Containing Reverse Micelles. *J. Solid-Phase Biochem.* 5:255–268.

27. Sheu, E., K. E. Göklen, T. A. Hatton, and S. H. Chen. 1986. Small-angle neutron scattering studies of protein-reversed micelle complexes. *Biotechnol. Prog.* 2:175–186.

28. Pereyra, P. M., E. Horvath, and P. E. Braun. 1988. Triton X-100 extraction of central nervous system myelin indicate a possible role for the minor myelin proteins in the stability of lamellae. *Neurochem. Res.* 13:583–595.